Electrical circuits on mesoscopic Sierpinski gaskets

2004 J. Phys. A: Math. Gen. 37 8823

(http://iopscience.iop.org/0305-4470/37/37/005)

INSTITUTE OF PHYSICS PUBLISHING JOURNAL OF PHYSICS A: MATHEMATICAL AND GENERAL

J. Phys. A: Math. Gen. **37** (2004) 8823–8833 PII: S0305-4470(04)80144-6

Electrical circuits on mesoscopic Sierpinski gaskets

R Burioni, D Cassi and F M Neri

Istituto Nazionale Fisica della Materia (INFM), Dipartimento di Fisica, Università di Parma, Parco Area delle Scienze, 7A 43100 Parma, Italy

E-mail: burioni@fis.unipr.it, cassi@fis.unipr.it and neri@fis.unipr.it

Received 3 May 2004
Published 1 September 2004
Online at stacks.iop.org/JPhysA/37/8823
doi:10.1088/0305-4470/37/37/005

Abstract

A deterministic network of impedances on the Sierpinski gasket fractal is considered, with particular regard to low-generation, or mesoscopic, systems. We study the fractal set of the resonances of the circuit and present calculations on frequency-dependent systems. The condition of an intermediate size can lead to an oscillatory scaling of the total impedance that disappears in the asymptotic limit: several examples are given.

PACS numbers: 64.60.Ak, 05.45.Df, 84.30.Bv

1. Introduction

The initial interest in the electrical properties of fractals was motivated by the need to explain the features of existing systems, such as the dielectric properties of percolating clusters or the ac response of some heterogeneous systems [1, 2]. More recently, physicists and electrical engineers [3] have recognized the self-similarity of fractals as a useful tool for engineering new devices, and exploited it to design fractal antennas [4], fractal diffraction gratings [5], fractal photonic bandgap slabs [6]. While the former research field involved the study of very big model systems (i.e. fractals with generation $n \to \infty$), the latter typically deals with low-size and deterministic fractals.

The most studied among these systems is by far the Sierpinski gasket. The problem of resistor networks on such a fractal has been the object of many studies, aimed at explaining the dc transport properties of the percolation backbone [1]. The more general issue of a network of complex impedances has been examined some years ago by several authors (see in particular the comprehensive review by Clerc *et al* [2]) that were almost exclusively interested in the percolative side of the problem, i.e. that relating to the ac dielectric response of inhomogeneous materials. Therefore they examined the critical behaviour ($n \to \infty$) of the system and found its critical exponents.

0305-4470/04/378823+11$30.00

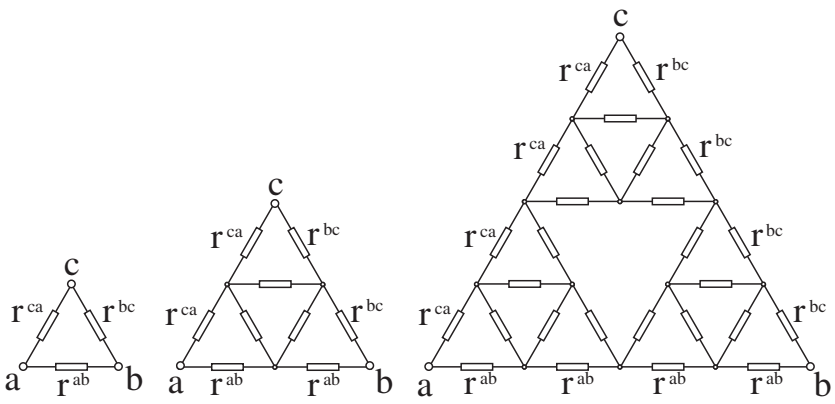

Figure 1. The Sierpinski gasket of impedances.

In the present paper we address the problem of mesoscopic networks of complex impedances on the Sierpinski gasket, namely, of systems of small size that stay away from the asymptotic regime. Since the networks we consider are relatively small and constituted by common passive elements such as resistors, inductors and capacitors, they can be easily reproduced in any electronics lab. Yet they display a highly nontrivial behaviour that comes as a direct consequence of the topology of the system and is lost in the thermodynamic limit.

The paper is organized as follows. In section 2 we obtain the decimation map for the network of impedances; we study its fixed points, asymptotic behaviour and invariant subspaces. In section 3 we study the distribution of poles of the map, that correspond to resonances of the fractal circuit. In section 4 we analyse the dependence on the frequency of the total impedance both for ideal ($n \to \infty$) and realistic ($n \to 1$) systems, and we stress the differences between the two cases. Section 5 studies the asymptotic behaviour of 'irregular' points of the map, and finds that their number is infinite, also connecting this feature to the results found in many other models on fractal systems. The conclusions are in section 6.

2. The map

We consider a fractal built from a triangle with an electrical pole on each of the three vertices a, b and c and 3 different (and in general complex) impedances r^{ab}, r^{bc}, r^{ca}, one at each link. The recursive rule for the construction of the fractal is shown in figure 1 (where we always call a, b and c the external poles).

We seek a decimation relation connecting the impedances of generation n to those of generation $n + 1$. The tool we shall use is the well-known 'star-triangle' transformation (or star-delta, or $Y - \Delta$ transformation [7]), which allows us to go from 'triangle' to 'star' variables and back by adding or subtracting a supplementary pole, as shown in figure 2. The variables r^{ab}, r^{bc}, r^{ca} and x, y, z are connected by simple algebraic relations, that we do not report here.

The procedure for the decimation of the gasket is outlined in figure 3; we omit the detailed calculation and give only the final result.

We will work with 'star' variables throughout. The map is:

$$x_{n+1} = \frac{3}{2}x_n + \frac{y_n z_n}{2(x_n + y_n + z_n)} \tag{1}$$

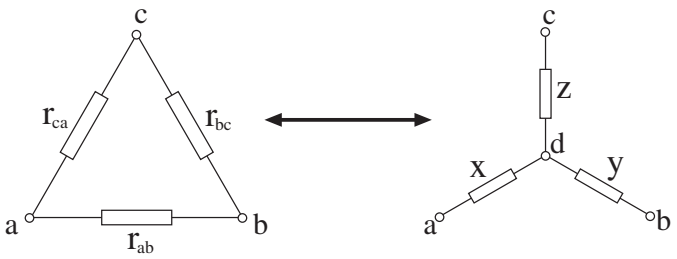

Figure 2. The star-triangle transformation: the 'triangle' (left) and 'star' (right) circuits are equivalent under a suitable choice of the variables.

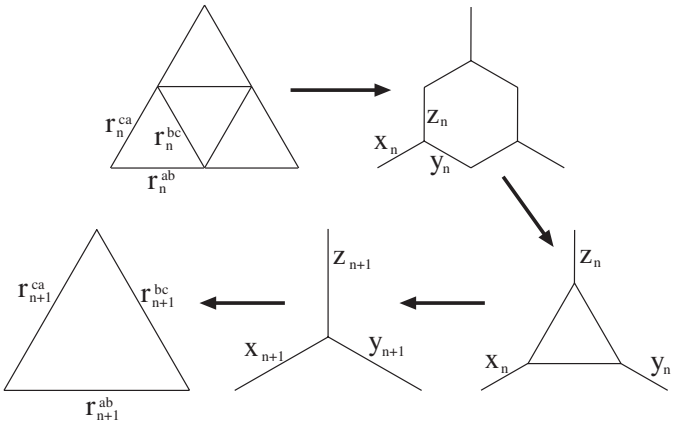

Figure 3. Decimation procedure for the Sierpinski gasket.

together with the two permutations $(x_n, y_n, z_n) \to (y_n, z_n, x_n) \to (z_n, x_n, y_n)$. We denote the map by T: $(x_{n+1}, y_{n+1}, z_{n+1}) = T(x_n, y_n, z_n)$.

It is a rational map of degree 2 from $\hat{\mathbf{C}}^3$ to $\hat{\mathbf{C}}^3$ (where $\hat{\mathbf{C}} = \mathbf{C} \cup \{\infty\}$). A main feature of the map is the invariance under any permutation of the variables x, y, z. As a consequence, the properties of a particular triple of impedances (x, y, z) also hold for all its permutations. Also, the properties of a particular one- or two-dimensional subspace (for instance a subspace with parametric equations $(x(t), y(t), z(t))$) are shared by all the subspaces obtained by permuting its equations (e.g. $(z(t), y(t), x(t))$). For the sake of conciseness, in such cases we will generally leave this fact implicit, treating only one permutation without mentioning the others. A second feature of the map T is that it is homogeneous of degree 1 in its variables: $T(\lambda x, \lambda y, \lambda z) = \lambda T(x, y, z)$, $\lambda \in \mathbf{C}$. We refer the reader to the specific literature [8] for the language of dynamical systems and rational maps.

An important remark: in the rest of the paper we will often talk about 'negative resistances'. Now, we recall that the only physical constraint on the impedance Z of a passive element (be it a resistance, capacitance, inductance or a combination of all three) is that its real part be non-negative: $\mathrm{Re}(Z) \geqslant 0$. So what does a 'negative resistance' (or negative real part) mean? A physical sense can be recovered from the fact that the map is homogeneous: if a result holds for the triple (x, y, z) it also holds for all the triples of the form $(\lambda x, \lambda y, \lambda z)$ with $\lambda \in \mathbf{C}$; so the result is 'physically meaningful' provided that there exists a $\lambda \in \mathbf{C}$ such that $\mathrm{Re}(\lambda x), \mathrm{Re}(\lambda y), \mathrm{Re}(\lambda z) \geqslant 0$. For instance, a triple of impedances such as $(-1, 1, 1)$

makes sense since it can be multiplied by an imaginary factor, say i, to give $(-\mathrm{i}, \mathrm{i}, \mathrm{i})$, that is a capacitance and two inductances. As a counterexample, the triple $(1+\mathrm{i}, -1+\mathrm{i}, -\mathrm{i})$ cannot be mapped by multiplication into any physically meaningful point.

Fixed points of the map. The vector space $(x, x, -x)$ (and permutations) is a line of repelling fixed points for T. The only attractive fixed point is the point at infinity $x_n \to y_n \to z_n \to \infty$ (except for subspace **II** that is discussed below). The series expansion of T near the fixed point gives the following asymptotic laws [2, 9]:

$$|x_n| \sim \left(\tfrac{5}{3}\right)^n \qquad |x_n - y_n| \sim \left(\tfrac{4}{3}\right)^n. \tag{2}$$

Invariant subspaces. There are 3 subspaces that are invariant under the application of T:

(i) $\boxed{z = y}$ The map is

$$x_{n+1} = \frac{3}{2}x_n + \frac{y_n^2}{2x_n + 4y_n} \qquad y_{n+1} = \frac{3}{2}y_n + \frac{x_n y_n}{2x_n + 4y_n}. \tag{3}$$

This will be the most extensively studied case.

(ii) $\boxed{z = -y}$ These are the points such that the impedance between the vertices b and c in figure 1 is always 0. In this subspace only the variable x evolves:

$$x_{n+1} = \frac{3}{2}x_n - \frac{y_n^2}{2x_n} \qquad y_{n+1} = y_n = y_0. \tag{4}$$

The fixed point of this subspace is $(\infty, y_0, -y_0)$; the asymptotic law is $|x_n| \sim (3/2)^n$, while the phase of x_n when $n \to \infty$ depends on the initial conditions.

(iii) $\boxed{x \in \mathbf{R}, \quad z = \overline{y}}$ In this case the impedance between b and c in figure 1 is real, while the other two are in general complex. Note that subspace **III** overlaps with subspace **I** when y and z are both real, and with subspace **II** when y and z are both imaginary; this is not a problem for the following discussion. Note also that for subspace **III** the homogeneity property is restricted to $\lambda \in \mathbf{R}$.

3. Poles of the map

The zeros and poles of the nth iterate of the map, $T^n(x, y, z)$, correspond to points where the impedance of the nth generation gasket is respectively zero or infinite, that is, to resonances of the nth generation circuit. Since the set of the zeros and the set of the poles share the same properties, we choose to focus on the poles.

We want to find the general structure of the backward orbit of the point ∞, that is, the set of the points $\mathcal{C} = \{(x, y, z) : T^n(x, y, z) = \infty \text{ for some } n\}$. We distinguish the order of the iterate of the map by calling $\mathcal{C}_n$ the set of the points (x, y, z) that are poles of the $(n+1)$th iterate: $\mathcal{C}_n = \{(x, y, z) : T^{n+1}(x, y, z) = \infty\}$, so that $\mathcal{C} = \bigcup_{n=0}^{\infty} \mathcal{C}_n$.

The set $\mathcal{C}_0$ consists of the points that make the denominator of T vanish, $T(\mathcal{C}_0) = \infty$, that is the plane $x + y + z = 0$. In order to find the set $\mathcal{C}_1$ we impose that $T(\mathcal{C}_1) = \mathcal{C}_0$ (so that $T^2(\mathcal{C}_1) = \infty$) and find the surface of equation $3x^2 + 3y^2 + 3z^2 + 7xy + 7xz + 7yz = 0$. We can proceed iteratively this way: at each step $T(\mathcal{C}_{n+1}) = \mathcal{C}_n$. In general $\mathcal{C}_n$ is a homogeneous algebraic surface of order 2^n and, due to the homogeneity, it is a generalized cone, the axis of which is the line $x = y = z$. The cone is best visualized by sectioning it with a plane orthogonal to its axis, which was done in figure 4 (here the plane is $x + y + z = 1$). The first 3 curves are shown on the left, while on the right we show the (numerically computed) full set of curves. Every $\mathcal{C}_n$ surface splits into 2^{n-1} distinct surfaces that intersect each other only at the vertex 0: the union set $\mathcal{C}$ therefore contains $2^n - 1$ distinct surfaces.

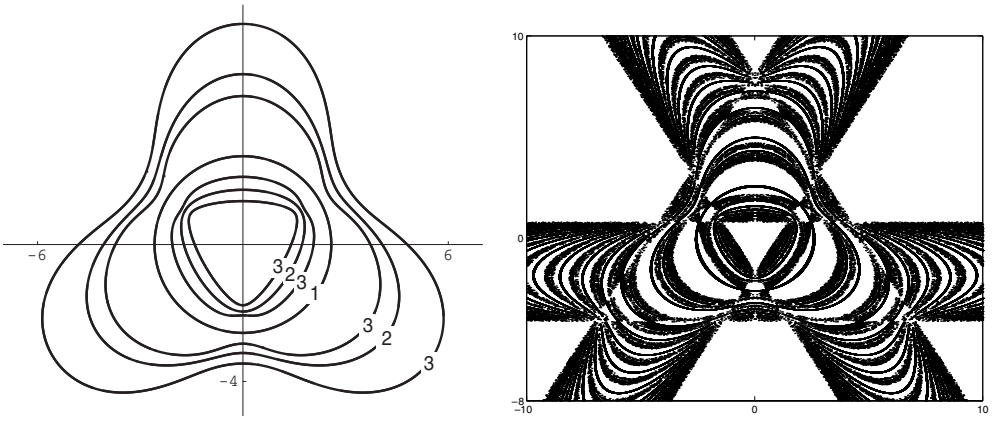

Figure 4. The cone $\mathcal{C}$ sectioned by the plane $x + y + z = 1$. Left: the intersection of the sets $\mathcal{C}_1, \mathcal{C}_2, \mathcal{C}_3$ (labelled 1, 2 and 3) with the plane. Right: the intersection of the whole set $\mathcal{C}$ with the plane. The triangle in the centre is the intersection of $\mathcal{C}$ with the octant $x, y, z > 0$. The threefold symmetry of the figure is apparent.

The set $\mathcal{C}$ is fractal, and thus its box-counting dimension can be computed (which could give an estimate of the complexity of our system with respect to regular circuits). We have computed it with numerical methods: it turns out to be $d_F = 2.82 \pm 0.03$.

4. Dependence on frequency

A practical way to implement the system above is to choose a generation n, put imaginary impedances (capacitors or inductors) on the basic cell and let the frequency vary, measuring the total impedance for each value of the frequency. For example we can choose two different inductances and one capacitance; the impedances of generation 0 are (in units i):

$$x_0 = \omega L_1 \qquad y_0 = \omega L_2 \qquad z_0 = -\frac{1}{\omega C}. \tag{5}$$

This can be seen as a parametric curve with parameter ω; the poles of the system are the intersections of the curve with the surface $\mathcal{C}$ introduced in the previous section. As above we define $\mathcal{C}_{\omega n}$ as the set of the frequencies that are mapped to infinity after n iterations of the map (the resonances of the system); we also define $\mathcal{C}_\omega = \bigcup_{n=0}^{\infty} \mathcal{C}_{\omega n}$. Since $\mathcal{C}$ is a homogeneous algebraic surface of order 2^n, $\mathcal{C}_{\omega n} = \{\omega : T^{n+1}(\omega L_1, \omega L_2, -1/\omega C) = \infty\}$ is a 2^n-degree algebraic equation in the unknown ω^2; thus (dropping negative solutions), $\mathcal{C}_{\omega n}$ consists of 2^n points along the positive real axis and a system of generation n has exactly $2^{n+1} - 1$ poles along the real axis.

The response of the system (that is, its total impedance) to a variable-frequency input is shown in figure 5 (left) for a very big system ($n = 50$). It is found that there is a fractal distribution of poles in a range of frequencies from 0 to the value $\tilde{\omega} = 1/\sqrt{C \cdot \tilde{L}}$, where $\tilde{L} = \min(L_1, L_2)$ (so for large n part of the information about the system, namely one of the Ls, is lost), while the response is smooth (without poles) for $\omega > \tilde{\omega}$. The high-frequency inductive behaviour ($Z \sim \omega$) can be recognized. For realistic systems ($n < 10$, so with a number of poles $<2^{10}$) the region with poles does not extend to 0 (figure 5, right); rather, the response becomes smooth for $\omega \to 0$ with a capacitive law ($Z \sim -1/\omega$). In the realistic case of a small non-zero real part of the impedances, the poles give place to resonance peaks, whose positions are roughly the same as those of the poles.

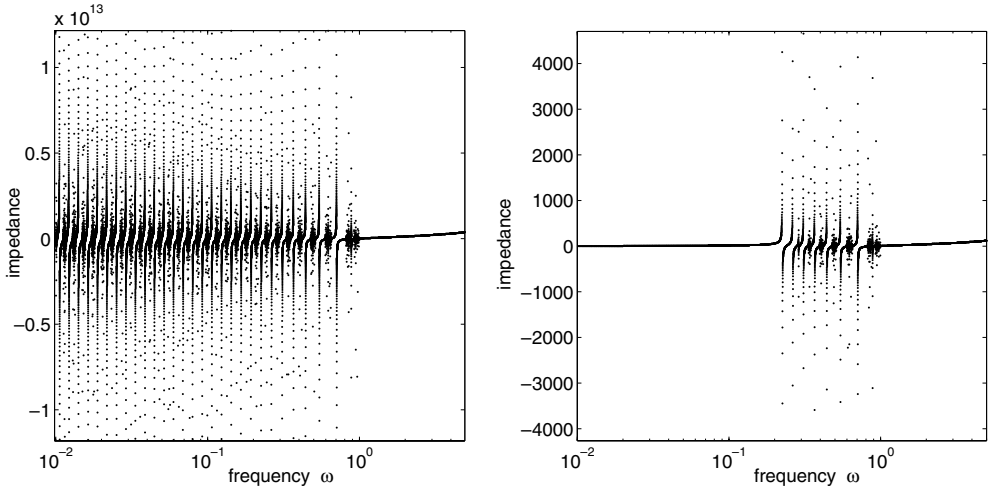

Figure 5. Frequency dependence of the total impedance (in imaginary units) for a basic cell with 2 inductances and a capacitor with values $C_1 = C_2 = L = 1$. Left: final impedance for a gasket of generation $n = 50$. Right: final impedance for a more realistic system with $n = 7$ (6561 links).

The positions of the poles, and thus of the smooth and the non-smooth regions, can be tuned by adjusting $L_{1,2}$ and C. However, it is found that the fractal dimension of the set $\mathcal{C}_\omega$ *does not depend* on the particular choice of $L_{1,2}$ and C. This is easily understood, since of the 3 parameters (a) the information about the value of the bigger of $L_{1,2}$ is lost, as we have seen, for $n \to \infty$; (b) another parameter can be factored out without changing the position of the poles and (c) the remaining one can be factored in ω, which results in a dilatation of the scale that does not affect the fractal dimension. The computed value of the fractal dimension of $\mathcal{C}_\omega$ turns out to be $d_F = 0.68 \pm 0.03$.

By choosing 2 capacitors and 1 inductance as the starting points ($x_0 = \omega L$, $y_0 = -1/\omega C_1$, $z_0 = -1/\omega C_2$) we get similar results. The response is smooth for $0 < \omega < \tilde{\omega}$, where $\tilde{\omega} = 1/\sqrt{\tilde{C} \cdot L}$ and $\tilde{C} = \max(C_1, C_2)$, and has a fractal distribution of poles for $\omega > \tilde{\omega}$ (figure 6, left). For systems with small n (figure 6, right) the non-smooth region does not extend to ∞ and the asymptotic law is inductive: $Z \sim \omega$.

Once again the fractal dimension of $\mathcal{C}_\omega$ does not depend on the values of L, $C_{1,2}$; we find $d_F = 0.56 \pm 0.02$.

5. Oscillating asymptotic behaviour

For the sake of simplicity we first restrict our examination to some invariant subspaces of the map; then we consider the general case.

5.1. Subspace I

We set $z = y$ and consider equation (3). We define the reduced variables $t_n = x_{n+1}/x_n$ and $u_n = y_n/x_n$; the new recursion relations read

$$u_{n+1} = \frac{6u_n^2 + 4u_n}{u_n^2 + 6u_n + 3} = U(u_n) \qquad t_{n+1} = \frac{3}{2} + \frac{u_{n+1}^2}{4u_{n+1} + 2}. \tag{6}$$

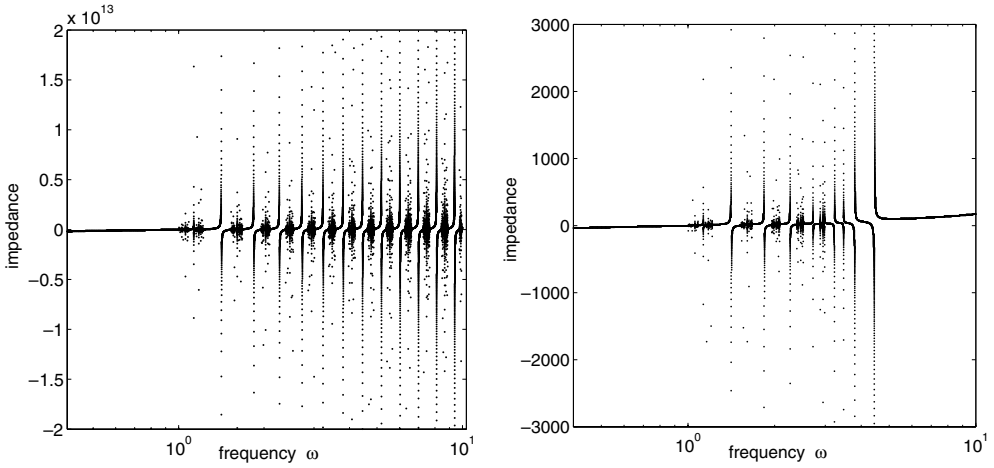

Figure 6. Frequency dependence of the total impedance (in imaginary units) for a basic cell with 2 capacitors and an inductance with values $L = C_1 = C_2 = 1$. Left: final impedance for a gasket of generation $n = 50$. *Right*: final impedance for the system with $n = 7$.

We have decoupled the variable u, that now evolves with its own monodimensional map U; furthermore, the variable t depends step by step on u only.

There are three fixed points for the map U, namely, -1 repelling (that corresponds to the line of repelling fixed points $x = -y$ of the map (3)), 1 attractive (corresponding to the attractive fixed point at infinity of the original map $x = y = \infty$), and 0 repelling (corresponding to any $y = 0$ for the map (3), which is of no physical interest since it amounts to two null impedances on the basic triangle).

Our main interest about the map U concerns the existence of periodic points. Suppose in fact that we have found a periodic point u_0 of period p: $u_p = U^p(u_0) = u_0$; from equation (6) we also get a periodic point for the map in t: $t_p = t_0$. Turning back to the original variables, from the periodicity of t we obtain

$$\frac{x_{p+1}}{x_p} = \frac{x_1}{x_0}; \qquad \frac{x_{p+2}}{x_{p+1}} = \frac{x_2}{x_1}; \qquad \cdots \frac{x_{2p}}{x_{2p-1}} = \frac{x_p}{x_{p-1}}; \tag{7}$$

and dividing term by term

$$\frac{x_p}{x_0} = \frac{x_{p+1}}{x_1} = \frac{x_{p+2}}{x_2} = (\cdots) = \frac{x_{p+k}}{x_k} \tag{8}$$

so for any positive integer m

$$x_{mp+k} = x_{(m-1)p+k}\left(\frac{x_p}{x_0}\right) = x_{(m-2)p+k}\left(\frac{x_p}{x_0}\right)^2 = (\cdots) \tag{9}$$

$$= \left(\frac{x_p}{x_0}\right)^m x_k, \qquad k = 0, 1, \ldots, p-1. \tag{10}$$

This means that the orbit of the system splits into p different branches, one for each of the first p points. All branches display the same power-law behaviour, $x_n \sim (x_p/x_0)^{\frac{n}{p}}$, but starting from a different point; at every step the system jumps from one branch to another: we call this *oscillating asymptotic behaviour* (OAB). In a logarithmic plot of x_n versus n this results in p different straight lines, as exemplified in figure 7 for $p = 3$. A compact form for the overall asymptotic law is

$$x_n \sim f_p(n)(a_p)^n \tag{11}$$

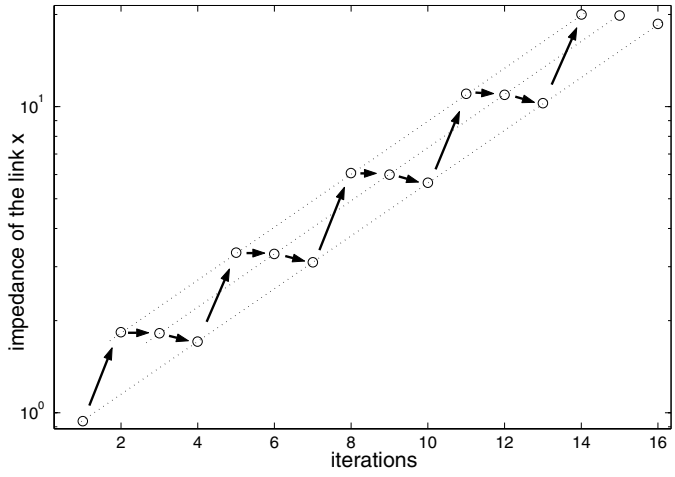

Figure 7. Example of oscillating asymptotic behaviour for $p = 3$.

where $a_p = (x_p/x_0)^{1/p}$ and $f_p(n)$ is a p-periodic function of n. The same asymptotic law holds for y_n and, therefore, for the total impedance.

We can prove that there are no attractive periodic points for the map U. In fact, if an attractive periodic point exists, then its basin of attraction contains at least one critical point (i.e., a point u such that $U'(u) = 0$) [8]. But the only two critical points of the map, $(1/16)(-9 \pm \mathrm{i}\sqrt{15})$, can be shown to belong to the basin of attraction of the fixed point 1. So, no attractive periodic point exists for any period p (there could possibly exist at most 2 irrationally indifferent periodic points, but we will not deal with this issue).

There are in general $2^p + 1$ periodic points of period p for the map (6) and it is easy to prove that they are all real. In fact they are a subset of the Julia set $J(U)$ of the map, i.e. the closure of the set of all repelling fixed points of the map U. Now, the following basic property holds for the Julia set [8]: suppose that $u_0 \in J(U)$; then $J(U)$ is equal to the closure of the set of all iterated preimages

$$\{u : U^n(u) = u_0 \text{ for some } n \geqslant 0\}.$$

So it is enough to look at *one* periodic point; for example we can take the repelling fixed point -1: by looking at the two preimages

$$U_{\pm}^{-1}(u) = \frac{-3u + 2 \pm \sqrt{6u^2 + 6u + 4}}{u - 6}$$

we see (figure 8) that they always lie between -1 and 0, and so does the whole backward orbit. So:

$$-1 \leqslant u_p \leqslant 0 \qquad \forall p$$

Being the Julia set infinite [8], the number of the periods p and of the values a_p is also infinite.

The existence of periodic renormalization group trajectories was recognized by McKay *et al* in a frustrated Ising model on some hierarchical lattices [10] that also exhibited period doubling cascade and chaotic behaviour; here we are dealing instead with periodic points of the map of the variables' *ratios*.

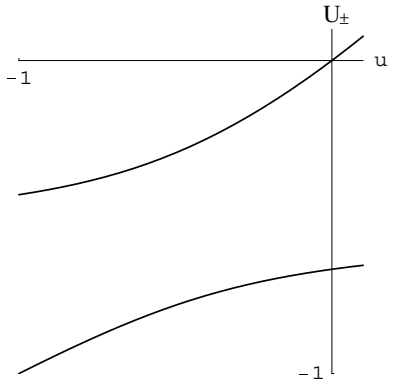

Figure 8. The two preimages of $U(u)$ between -1 and 0.

Derrida *et al* [11] discovered a phenomenon similar to that discussed in this section in statistical models on hierarchical lattices such as the diamond lattice; they called it 'oscillatory critical amplitudes' and connected its properties to the Julia set of the renormalization group map. Doucot *et al* [12] predicted and experimentally measured log-periodic oscillations of the magnetoresistance as a function of the magnetic field at low temperatures in a Sierpinski gasket network of submicronic Al thin wires. Today the presence of log-periodic corrections to scaling and complex exponents in statistical models is generally recognized as a consequence of the discrete scale invariance of the underlying lattice and is found in a variety of systems defined on fractals; see [13] for a review.

We stress that while the latter phenomena are found in statistical systems in the thermodynamic limit, the phenomenon discussed in this section is a unique feature of limited-size systems. Indeed it is found in correspondence with *repelling* periodic points of a rational map: since it is impossible to tune impedances with infinite precision on the repelling point, iterating the map will eventually drive the system away from the periodic orbit and lead it to its attracting fixed point. So the oscillating behaviour is lost in the thermodynamic limit.

5.2. Subspace II

From equation (4) we are led to consider the map

$$u_{n+1} = \frac{3}{2}u_n - \frac{1}{2u_n} \tag{12}$$

with $u_n = x_n/y_n = x_n/y_0$; its fixed points are ± 1 (repelling) and ∞ (attracting). The same considerations as in the previous section can be applied here. In particular we can prove that the Julia set of the map lies in the interval $[-1, 1]$ of the real axis, so the repelling periodic points are all real. There are no attractive periodic points since the only two critical points, $\pm i/\sqrt{3}$, fall in the basin of attraction of ∞. There are 2^p periodic points of period p (e.g., the periodic points of period 2 are $\pm 1/\sqrt{5}$). Due to the fact that y_n never changes its value, we are dealing with an oscillating asymptotic behaviour with $n = 0$, that is with periodic points of the map (4) itself.

5.3. Subspace III

In this case we are not able to find a decoupled equivalent system and are forced to look for the solutions of a nonlinear system of two coupled equations (see the general case below).

We find with numerical methods a set of 3-period complex points with the real (and possibly integer) ratio $a_3 = (x_3/x_0) = 15$; some of them are (setting $x_0 = 1$ for all points):

$$\begin{aligned} y_0 &= -0.445\,158 \pm 0.925\,134\ \mathrm{i} \\ y_0 &= -0.427\,766 \pm 0.448\,792\ \mathrm{i} \\ y_0 &= -0.749\,766 \pm 0.310\,933\ \mathrm{i} \end{aligned} \tag{13}$$

5.4. General case

In 3 dimensions starting from the map T (equation (1)) we define the reduced dimensionless variables $t_n = x_{n+1}/x_n$, $u_n = y_n/x_n$ and $w_n = z_n/x_n$; we are led to the new recursion relations

$$\begin{aligned} u_{n+1} &= \frac{3u_n^2 + 3u_n + w_n + 3u_n w_n}{3 + 3u_n + 3w_n + u_n w_n} \\ w_{n+1} &= \frac{3w_n^2 + 3w_n + u_n + 3u_n w_n}{3 + 3u_n + 3w_n + u_n w_n} \\ t_{n+1} &= \frac{3}{2} + \frac{u_{n+1} w_{n+1}}{2u_{n+1} + 2w_{n+1} + 2}. \end{aligned} \tag{14}$$

where we have decoupled the variables u and w, that evolve with their own map $(u_n, w_n) \to (u_{n+1}, w_{n+1})$, while the variable t depends step by step upon u and w. The considerations of the previous cases still hold: in order to find an OAB we have to seek a periodic point for the bidimensional map $(u_n, w_n) \to (u_{n+1}, w_{n+1})$. This is a much harder task than the previous, since it involves the solution of a nonlinear system of two equations: all we can say is that in general the number of periodic points of period p is *at most* 2^{p+1}. Indeed, most of the properties we exploited for the one-dimensional rational maps do not hold anymore for multidimensional maps; in particular, we are not able to find any bound for the Julia set.

If we exclude the points in common with any of the previous subspaces, we find no points of period 2 but some (complex) points of period 3 of the map $(u_n, w_n) \to (u_{n+1}, w_{n+1})$: for example

$$\begin{aligned} &(-1.213\,33 \pm 1.017\,55\ \mathrm{i},\ 0.755\,07 \mp 1.379\,73\ \mathrm{i}) \\ &(-0.925\,235 \pm 0.361\,205\ \mathrm{i},\ -0.483\,867 \mp 0.405\,791\ \mathrm{i}) \\ &(-0.937\,869 \mp 0.366\,138\ \mathrm{i},\ 0.305\,229 \pm 0.557\,741\ \mathrm{i}) \end{aligned} \tag{15}$$

The corresponding OAB of the map T has $a_3 = 1.6875 \pm 0.726\,184$ i.

6. Summary and conclusions

In this paper we considered the problem of a network of impedances on a Sierpinski gasket. The rational map associated with the renormalization of the network has been studied. The peculiar topology of the network gives rise to a fractal distribution of resonances in the impedance space; its fractal dimension has been calculated.

We have addressed the problem of the dependence on frequency of the response of the system. The response is smooth except in a range of frequencies, that depends on the initial conditions, where it shows a fractal distribution of resonances; its d_F has been determined for the most common cases. The difference between the thermodynamic limit and the more realistic mesoscopic cases has been highlighted.

The study of several related rational maps shows that there exist points whose evolution follows a power law modulated by periodic oscillations; the number of such points, of the power law exponents and of the period values is infinite. This phenomenon is quite similar to that found in other models on fractals and is usually referred to as log-periodic oscillations [13]. The main difference is that in statistical models the log-periodic corrections to scaling are a general feature of the asymptotic regime, arising from the underlying fractal structure. On the contrary, in our deterministic model the oscillating behaviour shows up in relatively small systems and disappears in the thermodynamic limit. Far from being a shortcoming, this peculiarity gives the phenomenon a strong chance of being observed in real, purpose-built systems.

We performed our calculations on the two-dimensional Sierpinski gasket: in doing so we were motivated by the common interest, shared by physicists and engineers, about its electrical properties. Anyway, the conditions under which we obtained our results do hold for many self-similar structures: therefore it is reasonable to ask in which other fractals such results remain valid. The closest nontrivial extension of our model is a network of impedances on the 3D version of the Sierpinski gasket: we expect it to display a richer behaviour, due to the higher number of degrees of freedom of its basic cell (6 versus 3) and to its higher degree of connectivity. This issue will be examined in a forthcoming work [14].

References

[1] Gefen Y, Aharony A, Mandelbrot B B and Kirkpatrick S 1981 *Phys. Rev. Lett.* **47** 1771

[2] Clerc J P, Giraud G, Laugier J M and Luck J M 1990 *Adv. Phys.* **39** 191

[3] Jaggard D L 1990 On fractal electrodynamics *Recent Advances in Electromagnetic Theory* ed H N Kritikos and D L Jaggard (New York: Springer)

[4] Puente C, Romeu J, Pous R, Garcia X and Benitez F 1996 *Electron. Lett.* **32** 1
Puente C, Romeu J, Pous R, Garcia X and Benitez F 2001 Fractal and space-filling transmission lines, resonators, filters and passive network elements *Patent* WO 01/54221
Gianvittorio J P and Rahmat-Samii Y 2002 *IEEE Antennas Propag. Mag.* **44** 20

[5] Lehman M 2001 *Opt. Commun.* **195** 11

[6] Weijia Wen, Lei Zhou, Jensen Li, Weikun Ge, Chan C T and Ping Sheng 2002 *Phys. Rev. Lett.* **89** 223901

[7] Frank D J and Lobb C J 1988 *Phys. Rev.* B **37** 302

[8] Blanchard P 1984 *Bull. Am. Math. Soc.* **11** 85
Beardon A F 1991 *Iteration of Rational Functions GMT 132* (New York: Springer)
Milnor J 2000 *Dynamics in One Complex Variable* 2nd edn (Braunschweig: Vieweg)

[9] Vannimenus J and Knežević M 1984 *J. Phys. C: Solid State Phys.* **17** 4927
Barlow M T, Hattori K, Hattori T and Watanabe H 1995 *Phys. Rev. Lett.* **75** 3042

[10] McKay S, Berker A N and Kirkpatrick S 1982 *Phys. Rev. Lett.* **48** 767

[11] Derrida B, Eckmann J-P and Erzan A 1983 *J. Phys. A: Math. Gen.* **16** 893
Derrida B, De Seze L and Itzykson C 1983 *J. Stat. Phys.* **33** 559
Derrida B, Itzykson C and Luck J M 1984 *Commun. Math. Phys.* **94** 115

[12] Doucot B, Wang W, Chaussy J, Pannetier B, Rammal R, Vareille A and Henry D 1986 *Phys. Rev. Lett.* **57** 1235

[13] Sornette D 1998 *Phys. Rep.* **297** 239

[14] Burioni R, Cassi D and Neri F M in preparation